Synthesis, and Docking Studies of Novel Heterocycles Incorporating the Indazolylthiazole Moiety as Antimicrobial and Anticancer Agents

Nadia Dawoud (dawoudnadia@yahoo.com)
Al-Azhar University
Hamada El-Gendi
City of Scientific Research and Technological Applications
Abdallah Abdallah
Al-Azhar University
Esmail M. El-Fakharany
City of Scientific Research and Technological Applications
Doaa Lotfy
Al-Azhar University

Research Article

Keywords: Anticancer, Antimicrobial, Molecular Docking, Indazole, Thiazole, Heterocycles

Posted Date: December 29th, 2021

DOI: https://doi.org/10.21203/rs.3.rs-1153610/v1

Abstract

The current study was directed toward developing a new series of fused heterocycles incorporating an indazolylthiazole moiety. The newly synthesized compounds were characterized through elemental analysis and spectral data (IR, ^{1}H-NMR, ^{13}C-NMR, and mass spectrometry). The cytotoxic effect of the newly synthesized compounds was evaluated against normal human cells (HFB-4) and cancer cell lines (HepG-2 and Caco-2). Among the synthesized compounds, derivatives 4, and 6 revealed significant selective antitumor activity, in a dose-dependent manner, against both HepG-2 and Caco-2 cell lines, with a lower risk toward HFB-4 cells (normal cells). Derivative **8** revealed the maximum antitumor activity toward both tumor cell lines, with an SI value of about approximately 26 and an IC_{50} value of approximately 5.9 µg/ml. The effect of these derivatives (8, 4, and 6) on the expression of 5 tumor regulating genes was studied through quantitative real-time PCR, where their interaction with these genes was simulated through a molecular docking study. Furthermore, the antimicrobial activity results revealed that compounds **2**, **7**, **8**, and **9** have potential antimicrobial activity, with maximum broad spectrum activity through compound **3** against the three tested pathogens: *Streptococcus mutans*, *Pseudomonas aeruginosa*, and *Candida albicans*. The newly prepared compounds also revealed antibiofilm formation activity with maximum activity against *Streptococcus mutans, Pseudomonas aeruginosa*, and *Candida albicans*.

1. Introduction

Cancer, one of the fundamental challenges for human health, represents the second causative agent of human mortality following cardiovascular diseases[1]. Recently, hepatocellular carcinoma and colorectal cancer were among the most dominant and high mortality rate cancer types[2, 3]. Hepatocellular carcinoma (HCC) is a worldwide health care issue that accounts for a high rate of mortality [3, 4]. Many factors are associated with HCC development, including chronic infections with hepatitis viruses (hepatitis B and C), aflatoxin exposure, obesity, and prolonged alcohol consumption[5, 6]. Currently, the only FDA-approved medication for HCC treatment is Sorafenib (a multikinase inhibitor), which can only extend patient survival for a brief time[7]. Although extrahepatic invasion of HCC outside liver cells is uncommon, growing evidence for rare colon metastasis with HCC treated only with surgical resection is lacking [8]. In the same context, colorectal cancer (CRC), characterized by a high mortality rate, represents the second leading cause of death among cancer-affected patients[9]. The current procedures applied for cancer prevention and treatment including radiation, chemotherapy, and surgery, are usually combined with immunosuppression for treated patients, which makes msusceptible omicrobial infections[10]. In addition, none of the applied treatments satisfy the requirements for selectivity and high efficacy toward cancer cells, and posttreatment side-effects are many and serious. Therefore, continuous research for developing highly selective new antitumor candidates with effective antimicrobial properties is a pressing demand toward an effective treatment for cancer patients[11].

In the last few decades, anticancer drugs have been developed from many chemically synthesized compounds [11, 12]. Heterocyclic derivatives, bearing at least two various elements, have attracted considerable attention in the growth of pharmacologically active molecules and advanced organic materials[13, 14], and represent over 75% of the current clinically applied drugs[15]. Among them, Sulfur, nitrogen, and/or oxygen-containing heterocyclic compounds, such as thiophene and pyrazole, always seek the attention of medicinal chemists and researchers attributed to their broad biological and pharmacological applications[16–18]. Thiophene has earned the sobriquet of the wonder heterocycle owing to the wide range of biological activities, such as anticancer[19–21], antimicrobial[22–24], antioxidant[25], and anti-inflammatory[26]. The name “thiophene” was derived from the Greek words ‘theion’ for sulfur and ‘phaino’ meaning shining[27]. Tiquizium bromides, tipepidine, tioconazole, and citizelam are among many marketed pharmaceutical drugs that contain thiophene nucleus[28–32]. Nevertheless, the low water solubility of thiophene in addition to series hepatotoxicity limits their wide application and even forces the removal of many thiophene-containing medicines from the drug market[33]. On the other hand, pyrazole is well known as a five-membered heterocyclic compound that has two neighboring nitrogen atoms, $C_3H_3N_2H$. Pyrazole derivatives have been applied for many years in agrochemicals as herbicides[34], and in the pharmaceuticals field as antimicrobial[35], anti-inflammatory[36], anticonvulsant[37, 38], and anticancer[39], with a recent application of pyrazole as a selective analgesic and anti-inflammatory drug (COX-2 inhibitor) has attracted more attention for these heterocyclic rings in medicinal chemistry[34]. With recent advances in molecular hybridization strategies, new structures could be developed toward a novel antitumor drug with lower cytotoxicity. This strategy is based upon combining pharmacophoric moieties of various bioactive compounds to develop a new potent hybrid compound with higher activity compared to the parent’s structures[40]. According to previous information, the present study concerns the synthesis and characterization of novel furan, thiophene, pyrazole, pyran, and pyridine derivatives from indazolylthiazolidinone moieties. In addition, their biological potentials, including antitumor and antimicrobial activities, were evaluated.

2. Results And Discussion

2.1. Chemistry and characterization

The pressing demand for highly selective novel anticancer drugs forces continuous research for developing new compounds toward an effective treatment for cancer-affected patients [11]. The molecular hybridization strategy of combining the active moieties from different compounds represents a promising tool for developing new structures with higher biological activity than their starting precursors[40]. In continuation of our search for novel heterocyclic chemistry-based anticancer, the suggestion, synthesis, and structure elucidation of some new heterocyclic systems (2-9) were realized using indazolylthiazolidin-4-one (1), which was prepared according to the literature[41]. Compound **1** was allowed to react with sulfanilamide[42], to produce the corresponding amino benzenesulfonamide derivative **2**, which in turn reacted with arylidinemalononitrile[43], to afford pyridine derivative **3** [Scheme 1]. IR, mass

spectrometry, and ^{13}C-NMR spectra were consistent with the proposed structures (cf. Expr section, Electronic Supplementary Material Fig. S1a and b, and Fig. S2 a, b and c).

On the other hand, compound **1** was employed in a series of experiments to investigate the reactivity of the ethenone group (COCH2) in the formation of the target fused heterocyclic system (4-9).

Compound **1** undergoes a reaction in refluxing ethanol containing a catalytic amount of piperidine and/or in dioxane containing triethylamine after being treated with malononitrile to afford furothiazole derivative **4** [Scheme 1]. The proposed structure of derivative **4** was confirmed by an IR spectrum, which revealed absorption bands at 3334-3215 and 2191cm^{-1}, demonstrating the presence of NH2 and CN functions, respectively, with concurrent disappearance of the carbonyl band. Its ^{13}C-NMR showed a signal at 115.53 ppm due to heteroaromatic (> CN) (see Electronic Supplementary Material Fig. S3 a, b and c). Furthermore, compound **1** was condensed with malononitrile[44, 45], to give the corresponding thienothiazole derivative **5** in a yield of 69% [Scheme 1]. The ^{13}C-NMR spectrum of derivative **5** demonstrated the presence of characteristic signals at 115.00, 161.55, and 171.60 ppm for (heteroaromatic> CN, C=N, S-C-N) (see Electronic Supplementary Material Fig. S4 a, b and c).

In the same manner, treatment of compound **1** with cyanoacetic acid hydrazide and elemental sulfur in dimethylformamide containing a catalytic amount of piperidine, gave another thienothiazole derivative **6** in 52% yield[Scheme 1]. The structures of the latter products were established based on the appearance of NH and NH2 absorption bands in the 3440, and 3324-3193 cm^{-1} regions and a nitrile function at 2190 cm^{-1} with the absence of the band corresponding to the ethenone carbonyl group (COCH2) in compound (**1)** in their IR spectra. The ^{1}H-NMR spectra revealed a singlet signal in the regions of 6.95 ppm and 7.80 ppm, which indicates the presence of thiophene NH2 protons exchangeable with D_2O. In addition to the characteristic singlet signal assigned to hydrazide NH protons at 9.60 ppm and another singlet signal at 4.30 ppm for hydrazide NH2 protons exchangeable with D_2O) (see Electronic Supplementary Material Fig. S5a and b).

The synthesis of compounds 5 and 6 takes place via the following mechanism:-

The proposed mechanism and pathway for conversion of indazolylthiazolidin-4 (compound 1) into the corresponding derivatives **5**, and **6**.

Moreover, treatment of compound **1** with ethyl cyanoacetate[46] led to the formation of a product that was assigned as thiazolopyran derivative **7** [Scheme 1]. The structure of (**7)** was substantiated by the IR spectrum, which displayed a characteristic band at υ = 1721 cm^{-1} assignable to the CO group of δ-lactone. Its ^{1}H-NMR spectrum displayed singlets at δ 3.88 ppm attributable to the CH2 pyran protons and at δ 8.40 ppm for C=NH (D_2O exchangeable) (see Electronic Supplementary Material Fig. S6 a, b and c).

Cyclocondensation of derivative (**1)** with cyanoacetic hydrazide in boiling ethanol containing drops of trimethylamine[47], yielded the corresponding pyrazolothiazole derivative **8** [Scheme 1]. The IR spectrum is

assignable to the NH, and C≡N groups as well as the absence of the CO group. The ^{1}H-NMR spectrum displayed a broad singlet at δ 3.39 ppm for CH2CN group protons with the presence of the characteristic absorption band at 2213cm^{-1} due to the CN group in its IR spectrum) (see Electronic Supplementary Material Fig. S7a and b).

Another thienothiazole (**9)** was synthesized via the reaction of (**1)** with ethyl chloroacetate and carbon disulfide in dioxane in the presence of anhydrous K_2CO_3[48], under reflux [Scheme 1]. The structure of product **(9)** was in agreement with its spectral and analytical data. For example, the IR spectrum revealed characteristic bands at 1731-1201 and 1028 cm^{-1} corresponding to CO and C=S groups. Its ^{1}H-NMR spectrum showed one triplet at δ1.18 ppm due to methyl ester, and one quartet due to methylene ester at δ 4.10 ppm (see Electronic Supplementary Material Fig. S8a and b).

2.2. Bioactivity of the synthesized indazolylthiazole-based heterocyclic compounds

2.2.1. Antitumor activity

The antitumor activity of the prepared derivatives was evaluated, in vitro, against HepG-2 (hepatoma) and Caco-2 (colon cancer) cells in comparison with normal human HBF-4 cells. Herein, the IC_{50} values of the synthesized derivatives against HFB-4 cells were calculated to range from 55.6-153.7 µg/ml (Table 1), indicating the significant safety of the prepared compounds toward normal human cells. On the other hand, the synthesized derivatives showed significant antitumor activity against both HepG-2 and Caco-2 cell lines with high SI values and low IC_{50} values. The results indicated that the two tumor, cell lines HepG-2 and Caco-2, showed nearly the same sensitivity against the tested compounds. Moreover, the antitumor activity of the synthesized derivatives occurred in a dose-dependent manner toward the tested cancer cells (Fig. 1). Our findings indicated that the synthesized derivative **8** showed superior antitumor activity toward both tested tumor cells indicated with an SI value of approximately 26, with very high selectivity toward tumor cells, as the IC_{50} values were nearly 5.9 µg/ml toward both HepG-2 and Caco-2 cell lines. Compound 8 was followed by derivatives **6** (21.8 for HepG-2 and 25.6 for Caco-2) and 4 (18.1 for HepG-2 and 23 for Caco-2), as indicated in Table 1. The superior antitumor activity of compound 8 could be attributed to the presence of a thiazolyl-pyrazole moiety, which per the literature exhibits strong anticancer activity [49–51]. In addition, the presence of acetonitrile, incorporated into the pyrazole ring (at position 3), may reveal anticancer activity, as reported through other authors[52, 53].

Table 1
The antitumor activity of the prepared derivatives against HepG-2 and Caco-2 cells compared with normal human HBF-4 cells expressed in IC_{50} (µg/ml) and SI values.

Cells	HFB-4	HepG-2		Caco-2	
Comp. No.	IC_{50}	IC_{50}	SI	IC_{50}	SI
1	65.21±2.99	6.50±0.16	10.03±0.46	9.69±0.29	6.73±0.31
2	110.8±1.54	6.37±0.36	17.39±0.24	6.06±1.26	18.28±0.25
3	55.59±1.58	7.72±0.38	7.20±0.20	7.74±0.81	7.18±0.20
4	142.3±1.48	7.88±0.10	18.06±0.19	6.18±1.14	23.03±0.24
5	97.66±2.41	7.57±0.36	12.90±0.32	7.59±0.24	12.87±0.32
6	133.2±4.18	6.12±0.19	21.75±0.03	5.21±0.22	25.59±0.03
7	104.8±6.20	9.53±0.32	10.99±0.65	9.20±0.27	11.39±0.67
8	153.7±1.76	5.86±0.34	26.23±0.30	5.89±0.38	26.08±0.30
9	65.65±0.29	5.23±0.25	12.55±0.06	5.95±0.10	11.04±0.05

The proportional morphological changes of HepG-2 and Caco-2 cells upon treatment with the three potent antitumor derivatives (4, 6, and 8) at different concentrations (4-16 µg/ml), were studied in a live-cell mode by inverted microscopy, and the effect of these derivatives on the tested tumor cells was elucidated(Fig. 2). The obtained images reveal that compounds **4**, **6**, and **8** enhance obvious cell damage and stimulate a clear alteration of the cell morphology in a dose-dependent manner. These cytotoxic modifications involved nuclear condensation and cell shrinkage with some blabbing effects. Based on these observed results, the antitumor activity of the tested compounds seems to be enhanced by apoptotic molecular mechanisms.

2.2.2. Evaluation of the effect of the newly synthesized derivatives on some tumor gene expression

The effect of the potent synthesized derivatives (4, 6, and 8) on five tumor regulating genes (β-catenin, VEGF, MMP-9, p53, and Bcl-2) was evaluated in both Caco-2 and HepG-2 cells using qRT‑PCR and compared to 5-FU as a standard antitumor drug. Compounds **4**, **6**, and **8** significantly downregulated the gene expression of VEGF, MMP-9, and Bcl-2 compared to 5-FU and untreated cells (Fig. 3). These data reveal that downregulation of Bcl-2 expression was certainly stimulated by more than 3-folds compared to control cells. Additionally, they significantly suppressed the expression of the β-catenin gene in both HepG-2 and Caco-2 treated cells, in contrast to 5-FU, which stimulated its expression. The β-catenin gene plays a major role in cell-cell adhesion in normal cells. Expression of this gene is under a strict regulation mechanism, where its overexpression is a main characteristic of cancer cells[54]. On the other hand, the expression level of p53 genes was dramatically upregulated by more than 2-8-fold in both treated HepG-2

and Caco-2 cells compared to control cells. p53 is an essential tumor- suppressor gene that triggers cell growth arrest and apoptosis, which are usually impaired in cancer cells[55]. Currently, p53 gene targeting is a promising tool for anticancer drugs[56]. The overexpression of p53 treated cells is in line with previous results (morphological changes study) showing that the applied derivatives induce apoptosis in cancer cells.

2.2.3. Cell cycle arrest analysis

Arresting of cell cycle phases was studied for the treated Caco-2 cells with the most potent compounds to advance insight into its potential cellular mechanism to induce the anticancer effect. For this target, Caco-2 cells were treated with compounds 4, 6, and 8 for 48 h. Figure 4 shows the capability of these compounds to induce arresting of cell cycle distribution in both main checkpoints phases (G0/G1 and G2/M) of cell population growth. Our finding reveal that the apoptotic phase (sub-G1) population becomes detectable after treatment. In addition, the synthesis (S) phase was decreased after treatment with all compounds, especially in the case of treatment with compound 8. Our significant results specify that the synthesized derivatives enhanced the cell cycle arrest of treated cells in both sub-G1 and S phases compared with untreated control untreated cells.

2.2.4. Molecular docking

Molecular docking analysis has been one of the most basic and important strategies for drug design and discovery[57]. To this end, the interaction and affinity of the newly prepared potent anticancer compounds (4, 6, and 8) toward five proteins; MMP-9, p53, β-catenin, Bcl-2, and VEGF, were simulated through molecular docking. The PDB IDs of these proteins used in the docking study are 4XCT, 3ZME, 1JDH, 2W3L, and 2XAC. The crystal structures were downloaded and prepared for docking of our compounds (Tables 2 and 3).

Table 2
Binding energies of the potent antitumor derivatives (4, 6, and 8) with the five examined proteins.

	4XCT	3ZME	1JDH	2W3L	2XAC
The ligand	-6.53	-6.82		-5.23	
Compound 4	-5.74	-4.45	-5.92	-4.95	-4.34
Compound 6	-5.81	-6.23	-5.26	-4.96	-4.62
Compound 8	-5.88	-5.15	-5.79	-4.91	-4.08

Table 3
The residues involved in the interaction of the potent derivatives (4, 6, and 8) with the five selected proteins.

	MMP-9 (4XCT)	p53 (3ZME)	β-catenin (1JDH)	Bcl-2 (2W3L)	VEGF (2XAC)
The ligand	Ala189[a]	Asp228[a]		Tyr67[a]	
	His236[a]	Thr 230[b]			
	Leu188[b]	Cys229[b]			
Compound 4	Ala189[a]	Cys220[a]	Asn430[a]	Glu95[a]	Gln27[a]
	Leu187[b]	Thr230[a]	Lys435[a]	Asp99[a]	
	His226[b]		Ser473[b]		
Compound 6	Ala189[a]	Pro151[a]	Lys435[a]	Glu95[a]	Gln27[a]
	Leu187[b]	Cys220[a]	Ser473[a]	Asp99[a]	Gln55[a]
	His226[b]	Asp228[a]	Arg474[a]		Pro28[b]
			Arg469[b]		
Compound 8	Tyr245[a]	Glu221[a]	Asn430[a]	Arg105[a]	Arg23[a&b]
	Arg249[a]		Lys435[a]		
	His236[b]		Arg474[a]		
			His470[b]		
			Arg515[b]		

The obtained data showed that our compounds were able to bind effectively to MMP-9 (PDB ID: 4XCT). We can see three essential residues to which the ligand binds. **Figure 5** reveals that the ligand formed two hydrogen bonds with Ala189 and His236 and one arene-H interaction with Leu188. Compound **4**, as well as compound **6**, showed a hydrogen bond with the essential amino acid Ala189. Moreover, two arene-H interactions with Leu187 and His226 were observed (**Fig. 6**), while compound **8** formed arene-H interactions with the essential residue His236. Furthermore, it exhibited two hydrogen bonds with Tyr245 and Arg249.

Concerning p53 (PDB ID 3ZME), the ligand showed one hydrogen bond with Asp228 and two arene-H interactions with Thr230 and Cys229. Compound **6** was found to be the most promising candidate. It exhibited a correct binding mode. In addition to its ability to form a hydrogen bond with the essential amino acid residue Asp228, it showed two further hydrogen bonds with Pro151 and Cys220 (**Figs. 7 and**

8). It also showed free binding energy (-6.32 Kcal/mol) nearly close to the ligand (-6.82 Kcal/mol). Compound **4** exhibited correct binding mode by forming two hydrogen bonds; one with the essential amino acid Thr230 and another with Cys220. Although compound **8** failed to form a hydrogen bond with an essential amino acid, it formed a hydrogen bond with Glu221.

Regarding β-catenin (PDB ID 1JDH), it was reported that the β-catenin residues His260, Asn261, Lys292, Ile296, Asp299, Tyr306, Gly307, Lys312, Lys335, Lys345, Arg376, Arg386, Asn387, Asn426, Cys429, Lys435, Cys466, His470, Arg474, and Lys508 are the residues that interact with TCF4 to form a complex[58,59]. Hence these residues are effective residues to which the inhibitor should bind. Our compounds showed interactions with more than one essential residue with binding energies ranging from -5.2 to -5.9 Kcal/mol. Hence they are expected to be effective inhibitors of β-catenin. Compound **8** was the best as it showed interactions with three effective residues; Lys435, Arg474, and His470. It formed hydrogen bonds with Lys435 and Arg474 and an arene-H interaction with His470. Moreover, it further exhibited a hydrogen bond with Asn430 and an arene-H interaction with Arg515 (**Fig. 9**). Compound **6** showed two essential hydrogen bonds with the effective residues Lys435 and Arg474. Furthermore, a hydrogen bond was formed with Ser473 and an arene-H interaction with Arg469 as illustrated in **Figure 10**. Compound 4 showed a hydrogen bond with the essential amino acid Lys435 and two hydrogen bonds with Asn430 and Ser473.

Regarding Bcl-2 (PDB ID 2 W3L), our compounds showed a binding manner that differed from that of the ligand. The ligand formed a hydrogen bond with Tyr67 to which no of our compounds bound, indicating that it is more likely that the studied compounds (4, 6, and 8) are not able to bind to this protein effectively.

Finally, the crystal structure of VEGF (PDB ID 2XAC) suggests that Gln27 is one of the effective residues involved in the binding of VEGF to VEGFR[60]. Compound **4**, as well as compound **6**, showed a hydrogen bond to Gln27. Compound **6** also demonstrated a further hydrogen bond with Gln55 and arene-H interaction with Pro28 (**Fig. 11**), while compound **8** interacted with Arg23 only.

2.2.5. Antimicrobial efficacy of the prepared compounds

The prevalence of drug-resistant pathogens highlights the need for novel antimicrobials with lower resistance induction potential[61]. In this direction, the antimicrobial activity of a series of novel prepared compounds (1-9) was assessed against three pathogens, including *Streptococcus mutans, Pseudomonas aeruginosa*, and *Candida albicans* using a microtiter-plate assay. The MIC results (Table 4) illustrated that **derivatives 7** and **8** revealed reasonable antibacterial activity against *Streptococcus mutans*, with maximum inhibition activity by derivative **3** indicated in the MIC value of 11.2 µg/ml, comparable to that of the ampicillin MIC (13.5 µg/ml). For gram-negative bacteria (*Pseudomonas aeruginosa*), derivatives 2 and 7 revealed moderate activities with maximum inhibition through **derivative 3** with MIC of 18.29 µg/ml, which is nearly the same as the applied reference ciprofloxacin MIC of 18.7 µg/ml. The newly prepared compounds revealed low to medium antifungal activity against *Candida albicans* with a maximum antifungal activity through compound **3** (MIC of 40.74 µg/ml), representing 36% clotrimazole

activity. In the scope of this study, among the newly peppered series, compound 3 revealed potent broad-spectrum antibacterial activity with moderate antifungal activity. The broad-spectrum antibacterial activity of compound 3 may be attributed to the incorporated thiazolopyridine moiety, which is accordant to[62]. Khidre et al., reported the broad-spectrum potency of the thiazolopyridine nucleus and its derivative against many human pathogens[63]. As per the literature[63], one of the possible mechanisms of the thiazolopyridine nucleus antimicrobial activity is through targeting and inactivating vital microbial enzymes such as DNA gyrase.

Table 4
The antimicrobial activity of the newly synthesized compounds represented in MIC (µg/ml) toward *Streptococcus mutant, Pseudomonas aeruginosa* and *Candida albicans*

Compound	*Streptococcus mutant*	*Pseudomonas aeruginosa*	*Candida albicans*
Ampicillin	13.5± 0.234	-	-
Ciprofloxacin	-	18.7± 0.475	-
Clotrimazole	-	-	14.5 ± 1.25
1	70.26 ±0.6919	71.39 ±2.281	86.59 ±1.211
2	49.71±0.5849	40.13±2.109	52.77±0.7862
3	11.12±0.4232	18.29±2.114	40.74±0.5511
4	34.41±0.2374	60.76±2.218	48.92±1.054
5	43.52±0.359	56.51±2.191	59.02±1.285
6	39.58±0.3478	58.47±2.267	57.3±1.32
7	22.42±0.3173	43.86±2.042	58.18±1.207
8	15.77±0.2052	53.05±2.183	56.17±1.235
9	48.77±0.2457	61.51±1.832	46.61±1.195

2.2.6. Microbial-biofilm inhibition activity

One of the key pathogenicity mechanisms for microbial pathogens is microbial biofilm formation, which supports the persistence of infection[64]. As a result, compounds that interfere with biofilm formation improve microorganisms' susceptibility to therapeutic drugs. To this end, the efficacy of the newly prepared compounds (**1-9**) was evaluated for inhibition of microbial biofilm formation using the TCP technique. The results **(**Fig. 12**)** revealed that compounds **3**, **4**, and **8** had antibiofilm formation activities against *Streptococcus mutans*, with maximum inhibition activity in compound **3** of approximately 64% (Fig. 12), whereas compounds **2**,**3**, **4**, and **5** revealed high potency in biofilm inhibition against *Pseudomonas aeruginosa* with a maximum biofilm inhibition through compound **2** of approximately

58.5%. In the case of *Candida albicans*, various preparations exerted antibiofilm activity, including compounds **3** (69%), **5** (68%), **6** (61%), and **7** (66%) with a maximum biofilm inhibition recorded through compound **9 of** nearly 79%.

3. Material And Methods

3.1. Chemistry and characterization

The melting point ranges were taken on a Gallenkamp electric melting point apparatus using the one end open capillary method and were uncorrected. IR spectra were recorded (KBr discs) on a Shimadzu FT-IR 8201 PC spectrophotometer.1 H NMR, and 13C NMR spectra, were recorded on a Bruker 300 spectrometer, using DMSO as the solvent and tetramethylsilane (TMS) as an internal reference.

3.1.1. Synthesis of 4-(2-(3-phenyl-1,3,4,5,6,7-hexahydro-2H-indazol-2-yl)thiazol-4-yl) amino) benzene sulfonamide (2).

An ethanolic solution of compound **1** (0.01mol, 3 gm) containing a catalytic amount of triethylamine, and sulphanilamide (0.01mol, 1.8 gm) was heated under reflux for 12 h, cooled to RT, and acidified by HCl. The solid formed was filtered off, washed with water, and purified by recrystallization from petroleum ether to give the required product **2** as a yellow powder in 53% yield, m. p 120-123^{o}C. Requires: C, 58.26; H, 5.11; N, 15.44; S, 14.14. Found: C, 58.07; H, 4.99; N, 15.29; S, 14. 02. IR (KBr): v (cm^{-1})1154 SO2, 1598C=C, 1627C=N, 2933, 2857CH-Al, 3025CH-Ar, 3377, 3200 cm^{-1} of NH2. MS m/z (%): m/z 453 (M^{+}, 14.16), 54 (100).

3.1.2. Synthesis of 4-(5-amino-6-cyano-7-phenyl-2-(3-phenyl-1,3,4,5,6,7-hexahydro-2H-indazol-2-yl) thiazolo[4,5-b]pyridin-4(7H)-yl)benzenesulfonamide (3).

A mixture of 4-(2-(3-phenyl-1,3,4,5,6,7-hexahydro-2H-indazol-2-yl)thiazol-4-yl)amino) benzene sulfonamide (**2**) (0.01mol,4.5 gm) and arylidine malononitrile (0.01mol,1.6 gm) in ethanol (20 ml) containing a catalytic amount of triethyl amine was heated under reflux for 12 h, cooled to RT, and acidified by HCl. The solid formed was filtered off, washed with water and purified by recrystallization from petroleum ether to give product **3** as a brown powder, in 73% yield, m. p 140-143^{o}C. Requires: C, 63.24; H, 4.81; N, 16.13; S, 10.55; Found: C, 63.05; H, 4.69; N, 16.00; S, 10.34. IR (KBr): v (cm^{-1}) 1156 SO2, 1628 C=N, 2198 CN, 2933CH-Al, 3025CH-Ar, 3340, 3214 NH2. ^{1}H-NMR(300 MHz,DMSO-d6): δ1.61-2.49 (8H,m,4CH2);5.35(2H,s,br,SO2NH2);7.27-7.90(14H,m,ArH+NH2);8.40(1H,s,br,NH). ^{13}C-NMR (100 MHz, DMSO-d6):δ22.51, 25.32, 27.45(4CH_2); 112.70, 122.00, 125.91, 126.66, 127.62, 128.26, 128.57, 128.70,

129.34, 138.05, 142.11, 154.35 (aromatic >C=C) and 118.02, 161.50, 164.05(heteroaromatic >C≡N, C-N, -C=N).

3.1.3. Synthesis of 5-amino-2-(3-phenyl-1,3,4,5,6,7-hexahydro-2H-indazol-2-yl)furo[2,3-d] thiazole-6-carbonitrile (4).

A mixture of derivative **1** (0.01mol,3 gm) and malononitrile (0.01mol,0.7gm) in dioxane (30 ml) containing catalytic amount of triethyl amine (1 ml), and/or in ethanol (25 ml) containing catalytic amount of piperidine (0.5 ml) was heated under reflux for 5 h, cooled to RT, and acidified by HCl. The solid precipitate was filtered off, washed with distal water (3 times) and recrystallized from dioxane to give compound **4** as a brown powder (52% yield), m. p 130-133^{o}C. Requires: C, 62.79; H, 4.71; N, 19.27; S, 8.82; Found: C, 62.65; H, 4.61; N, 19.03; S, 8.72. IR (KBr): v (cm^{-1}) 1553C=C, 1627C=N, 2191 CN, 2935CH-Al, 3058CH-Ar, 3333, 3201NH2. ^{1}H-NMR(300 MHz,DMSO-d6):δ1.66-2.49(8H,m,4CH_2); 4.09(2H,s,br,CH); 6.87 (2H,s,br, NH2)exchangeable with D_2O; 7.20-7.74(5H,m,Ar-H); 8.15(1H,s,NH). ^{13}C-NMR (100 MHz, DMSO-d6): δ21.25, 22.04, 25.84, 26.60(4CH_2); 98,108,120.60, 126.82, 127.40, 128.23, 129.01, 129.40, 130.18, 142.93 (aromatic >C=C); 115.53, 162.0 5 (heteroaromatic > C≡N, N-C=N).

3.1.4. Synthesis of 5-amino-2-(3-phenyl-1,3,4,5,6,7-hexahydro-2H-indazol-2-yl)thieno[3,2-d]thiazole-6-carbonitrile (5).

The ethanolic solution of derivative **1** (0.01mol, 3 gm) containing catalytic amount of piperidine (0.5 ml), malononitril (0.01mol, 0.7 gm), and sulphur element (0.01mol, 0.3 gm) was heated under reflux for 4 h, filtered off on hot to get rid of an excess of sulphur, cooled to RT, and acidified by HCl. The separated solid was filtered off, washed with water and purified by recrystallization from toluene to give derivative **5** as a brownish red powder, in 69% yield, m. p 135-137^{o}C. Requires: C, 60.13; H, 4.52; N, 18.45; S, 16.90, Found: C, 60.00; H, 4.42; N, 18.39; S, 16.69. IR (KBr): v (cm^{-1}) 1561 C=C, 1621C=N, 2190 CN, 2857, 2935CH-Al, 3025, 3057CH-Ar, 3324, 3193NH_2. ^{1}H-NMR (300 MHz, DMSO-d6):δ1.56-2.49(8H, m, 4CH2); 4.25(2H, s, br, CH); 6.95(2H, s, br, NH2) exchangeable with D_2O; 7.12-7.97 (5H, m, Ar-H+CH-thiazole); 8.45 (1H, s, indazole). ^{13}C-NMR (100 MHz, DMSO-d6): δ 22.18, 23.65, 24.65, 26.33(4CH2); 112.55, 115.00, 118.00, 125.23, 127.57, 128.20, 129.52, 143.05, 144.32, 161.55, 171.60 (aromatic >C=C) and (heteroaromatic>C≡N, N-C=N, S-C-N).

3.1.5. Synthesis of 5-amino-2-(3-phenyl-1,3,4,5,6,7-hexahydro-2H-indazol-2-yl)thieno[3,2-d] thiazole-6-carbohydrazide (6).

A mixture of compound **1** (0.01mol, 3gm), cyanoacetichydrazide (0.01mol, 1gm), and Sulphur element (0.01mol,0.3 gm) in dimethyl formamide (20 ml) containing a catalytic amount of piperidine (0.5 ml), was

heated under reflux for 12 h, filtered off hot to get rid of an excess of Sulphur, cooled to RT, and acidified by HCl. The solid formed was filtered off, washed with water, and purified by recrystallization from petroleum ether to give product **6** as a brownish-red powder, in 52% yield, m. p 160-163^{o}C. Requires: C, 55.32; H, 4.89; N, 20.37; S, 15.54; Found: C, 55.27; H, 4.80; N, 20.29; S, 15.49. IR (KBr): v (cm^{-1}) 1493 C=C, 1621 C=N, 2858, 2932 CH-Al, 3025, 3058CH-Ar, 3.350, 3195NH2. ^{1}H-NMR(300 MHz, DMSO-d6):δ1.64-2.33(8H,m,4CH2); 4.30(2H,s,br, NH2NH)exchangeable with D_2O; 4.55(1H,s,CH) ;7.15-7.50(5H,m,Ar-H);7.80(2H,s,NH2) exchangeable with D_2O; 9.75 (1H,s,NHNH2) exchangeable withD_2O.

3.1.6. Synthesis of 7-i mino-2-(3-phenyl-1,3,4,5,6,7-hexahydro-2H-indazol-2-yl)-6,7-dihydro-5H-pyrano [2,3-d]thiazol-5-one (7).

A mixture of derivative **1** (0.01mol, 3 gm) and ethyl cyanoacetate (0.01mol, 1.2 gm) in dioxane (30 ml) containing a catalytic amount of piperidine (0.5 ml) was heated under reflux for 5 h, cooled to RT, and acidified by HCl. The separated solid was filtered off, washed with water and purified by recrystallization from benzene to give the required product **7** as a brown powder, in 37% yield, m. p 95-98 ^{o}C. Requires: C, 62.28; H, 4.95; N, 15.29; S, 8.75. Found: C, 62.11; H, 4.89; N, 15.18; S, 8.68. IR (KBr): v (cm^{-1}) 1547C=C, 1626C=N, 1721C=O, δ-lactone, 2935 CH-Al, 3025CH-Ar, 3345 NH. ^{1}H-NMR(300 MHz,DMSO-d6): δ1.67-2.49(8H,m,4CH2); 3.88(2H,s,br,CH2-pyran); 7.22-7.52(5H,m,Ar-H); 8.15,8.40 (2H,s,2NH) with D_2O exchangeable.^{13}C-NMR(100 MHz, DMSO-d6):δ*21.85*, 23.59, 24.45,26.33 (4CH2) ; 62(CH2-pyran ring); 94.40(CH-pyrazole); 120.49, 12517, 125.66, 126.76,127.19, 128.24,129.30, 130.91,131.98,133.39, 135.77,146.34, 151.44 ,155.09, 156.20 (aromatic >C=C) and (heteroaromatic > NHC= 706; N-151 C).

3.1.7. Synthesis of 2-(1-amino-5-(3-phenyl-1,3,4,5,6,7-hexahydro-2H-indazol-2-yl)-1H-pyrazolo [3,4-d] thiazol-3-yl)acetonitrile (8).

An ethanolic solution of derivative **1** (0.01mol, 3 gm) containing a catalytic amount of piperidine (0.5 ml), and cyanoacetichydrazide (0.01mol, 1 gm) was heated under reflux for 12 h, cooled to RT, and acidified by HCl. The solid formed was filtered off, washed with water and purified by recrystallization from toluene to give product **8** as a pale brown powder, in 70% yield, m. p 170-173 ^{o}C. Requires: C, 60.46; H, 5.07; N, 25.98; S, 8.49; Found: C, 60.39; H, 4.89; N, 25.87; S, 8.37. IR (KBr): v (cm^{-1}) 1493C=C, 1628C=N, 2213CN, 2857, 2933CH-Al, 3025, 3057CH-Ar, 3191NH. ^{1}H-NMR(300 MHz, DMSO-d6):δ1.59-2.97(8H,m,4CH2); 3.39(2H,s,br,CH2); 7.27-7.86(5H,m,Ar-H); 10.63(1H,s, NH-pyrazole).

3.1.8. Synthesis of ethyl 2-(3-phenyl-1,3,4,5,6,7-hexahydro-2H-indazol-2-yl)-6-thioxo-6,6a-dihydrothieno [3,4-d]thiazole-4-carboxylate (9).

A mixture of compound **1** (0.01mol, 3 gm), ethyl chloroacetate (0.01mol, 1.2 gm), and carbon disulfide (0.01mol, 0.8 gm) in dry dioxane (30 ml) containing anhydrous K_2CO_3 (2 gm) was stirred at RT for 12 h, and filtered off to remove excess K_2CO_3. The filtrate was poured onto ice water. The precipitate was filtered out, washed three times with deionized water and purified by recrystallization from benzene to give the required product **9** (orange powder) in 32% yield, m. p 85-88 ^oC. Requires: C, 56.86; H, 4.77; N, 9.47; S, 21.68. Found: C, 56.76; H, 4.70; N, 9.38; S, 21.58. IR(KBr):v(cm^{-1})1028C-S, 1205C=S, 1583C=C, 1621C=N, 1731C=O, 2858,2932CH-Al, 3025, 3057CH-Ar, 3411NH. ^{1}H-NMR (300 MHz,DMSO-d6): δ1.18(3H,t, CH2 CH3);1.62-2.31(8H,m,4CH2); 3.99(1H,s,CH); 4.12 (2H,q,CH2CH3); 4.50(1H,CH); 7.12-7.86 (5H,m,Ar-H); 8.55(1H,s,NH).

3.2. Evaluating the biological activities of the newly synthesized compounds

3.2.1. Cytotoxicity and antitumor activity evaluation

The human melanocytes (HFB-4) cells, hepatoma (HepG-2) cells, and colon carcinoma (Caco-2) cells were obtained from American Type Culture Collection (ATCC, USA). The cytotoxicity of the newly synthesized compounds (at different concentrations) was evaluated against HFB-4 cells (normal human melanocytes), HepG-2 cells (hepatoma), and Caco-2 cells (colon carcinoma) by using the 3-[4, 5-dimethylthiazol]-2, 5-diphenyltetrazolium bromide method (MTT assay) [65]. Normal and cancer cells (1.0×10^4) were cultured in sterile 96-well microplates, incubated for 24 h in DMEM (Lonza, USA) supplemented with 10% fetal bovine serum (Gibco, USA) for HFB-4 and Caco-2 cells or in a RPMI-1640 medium (Lonza, USA) supplemented with 10% FBS for HepG-2 cells. After 24 h of incubation, different doses of the tested synthesized compounds (2-64 g/ml) were added in triplicate to all cells and incubated for another 48 h in 5% CO_2. After washing the cells 3 times with fresh media, to remove dead cells and debris, a solution of MTT (Sigma Aldrich, 0.5 mg/ml) was added to each well and incubated for 2-5 h at 37°C. Afterward, the MTT solution was decanted and 200 µl of DMSO was added. The optical density was measured at 570 nm using a microplate reader (BMG LabTech, Germany), where the cells' relative viability (%) was estimated using the following equation:

Viability of cells (%) = $[A_1\text{-}A_0/A_U\text{-}A_0] \times 100$, where A1 is the absorbance of the test compound, A_0 is the absorbance of the blank, and A_U is the absorbance of untreated cells (control).

The antitumor activity of the synthesized compound was determined by calculating the IC_{50} value (half maximal inhibitory concentration) using Graph Pad Prism 6.0 software. The value of IC_{50} indicates the derivative concentration that causes 50% cell death, whereas the value of the selectivity index (SI), indicating the ratio of the IC_{50} value of normal cells versus the IC_{50} value of tumor cells, was also included as reported by[66, 68]. Furthermore, the effect of the highly active antitumor derivatives (4, 6, and 8) on the morphology of HepG-2 and Caco-2 cells was explored at different concentrations (4-16 µg/ml)

by using phase-contrast microscopy (Olympus, Germany) and compared to untreated cells (negative control).

3.2.2. The influence of the newly synthesized derivatives on the expression level of some tumor regulating genes

The effect of the potent antitumor derivatives (4, 6, and 8) on the expression level of some tumor regulating genes was elucidated through quantitative real-time PCR (qRT- PCR) and compared to that of a 5-fluorouracil (5-FU) reference antitumor drug. Five genes were assessed, including the tumor oncogene (Bcl-2), tumor suppressor gene (p53), matrix metalloproteinase gene (MMP-9), vascular endothelial growth factor gene (VEGF), and beta-catenin protein gene (B-catenin), in HepG-2 and Caco-2 cells, before and after treatment for 2 days with IC_{50} concentrations for compounds 4, 6, and 8. Following the extraction of total RNA from the tested cells, using the Gene JET RNA Purification Kit (Thermo Scientific, USA), cDNA synthesis was performed according to the protocol of the cDNA Synthesis Kit (Thermo Scientific, USA). qRT PCR was performed using the SYBR green kit and specific primers (Forward/Reverse) as follows: 5'-TCCGATCAGGAAGGCTAGAGTT-3'/5'-TCG GTCTCCTAAAAGCAGGC-3' for the Bcl-2 gene, 5'-TAACAGTTCCTGCATG GG CG GC- 3'/ 5'-AGGACAGGCACAAACACGCACC-3' for p53, 5'-CTGCGTATTTCCATT CATC-3'/ 5'-CCTTGGGTCAGGTTTAGAG-3' for the MMP-9 gene, 5'-GGCTTTACT GCTGTACCTCC-3'/5'-CAAATGCTTTCTCCGCTCT-3' for the VEGF gene, and 5'-CATATGCGGCTGCTG TTCTA-3'/ 5'-CCGAAAG CCGTTTCTTGTAG-3' for the β-catenin gene. The upregulation and/or downregulation of the expression of the tested genes in Caco-2 and HepG-2 cells was determined by using the equation $2^{-\Delta\Delta CT}$ [66].

3.2.3. Cell cycle arrest analysis

The cell cycle arrest of treated Caco-2 cells was evaluated through flow cytometry (Partec, Germany) in comparison with untreated cells and treated cells with 5-FU as a positive control [42–44]. After treatment of Caco-2 cells with the most potent compounds at IC_{50} concentrations, the cells were resuspended in 1 ml of cold PBS, pH, 7.2. After washing the cells three times, the cells were fixed by adding 1 ml of 70% cold ethanol dropwise with a gentle vortex. Caco-2 cells were washed three times again with cold PBS and incubated in 1 ml of PBS containing 5 µg/ml RNase A (Sigma-Aldrich) for 1 h at 37°C. Then 10µl of PI (Sigma-Aldrich) was added to cells at a final concentration of 1 mg/ml in deionized water and left at 4°C until analysis in the dark. The cell cycle of Caco-2 cells before and after treatment was analyzed by FACS using Cell Quist and Mod Fit software by reading at 488 nm.

3.2.4. Molecular Docking Analysis

Molecular Operating Environment (MOE 2014) software was used to simulate the binding orientations and interactions of the potent antitumor derivatives (4, 6, and 8) into five tumor regulating proteins namely MMP-9, p53, β-catenin, Bcl-2, and VEGF. The three-dimensional structure of the selected proteins was downloaded from the PDB website. The water molecules and repeated chains were removed.

Protons were added and the energy of the protein was minimized. The isolation of the pocket was then carried out. Validation of the downloaded structure was confirmed by redocking the downloaded ligand into the isolated pocket. The obtained root mean square deviation (RMSD) was found to be lower than 1.5 Å. The preparation of potent antitumor derivatives (4, 6, and 8) for docking was carried out by the construction of chemical structures at the MOE. Protons were then added to the 3D structure. Finally, the energy was minimized using Force Field MMFF94x. The prepared structures were added to the created database. MOE conducted the docking of the newly synthesized compounds, calculated the binding energies, and provided the binding modes of them[11].

3.2.5. Evaluation of the antimicrobial activity of the prepared compounds

The antimicrobial activity of the newly synthesized compounds **(**1-9**)** was evaluated against three pathogenic microorganisms as follows: *Streptococcus mutans* ATCC 25175 (Gram-positive); *Pseudomonas aeruginosa* ATCC 27853 (Gram-negative); and *Candida albicans* ATCC 10231 (fungi-like unicellular organism). After cultivating the three tested pathogens overnight in LB broth, 100 µl of each tested organism (106 CFU/ml) was added separately to 100 µl of the serially diluted test compounds (5-80 µg) in a 96-well tissue culture plate, and incubated at 37°C for 24 h. Eventually, microbial growth was measured at 600 nm, and the results are presented in the form of MIC (Table 4). Two antibacterial reference drugs, ampicillin and ciprofloxacin, and one antifungal drug, clotrimazole, were incorporated into the experiments.

3.2.6. Evaluation of the activity of the newly synthesized derivatives on microbial-biofilm inhibition

The activity of the newly synthesized compounds against microbial biofilm formation was estimated through the tissue- culture plate technique (TCP) as follows: the three abovementioned pathogens, *Streptococcus mutans*, *Pseudomonas aeruginosa*, and *Candida albicans* were cultivated overnight in LB broth at 37°C. Afterward, 200 µl of each diluted organism (10^6 CFU/ml) was inoculated separately (in triplicate) into 96-well tissue- culture plates and incubated overnight at 37°C. Following the incubation period, the free planktonic cells were removed by flipping the plate and washing each well three times with phosphate-buffered-saline (PBS), pH 7.1. To each well, 175 µl of fresh LB broth was added along with 25 µl of the tested compound (25 µg/ml final concentrations). The plates were reincubated at 37°C for another 24 h, washed with PBS buffer pH 7.1 three times and dried for 5 min at 50°C. The formed biofilm was stained with crystal violet solution (0.1% w/v) for 5 min. The excess stain was decanted, and the stained biofilm was solubilized with 200 µl of glacial acetic acid (30% v/v), where the developed blue color was measured at 590 nm. The results are expressed as relative inhibition (%) compared to untreated groups (control). Controls were prepared by culturing the three pathogens on LB medium without any tested compounds.

3.2.7. Statistical analysis

All experiments were performed in triplicate (n = 3), and all data are expressed as the mean ± SEM. Significance of statistical analysis was evaluated by the multiple comparisons Tukey's post-hoc test of the one-way analysis of variance (ANOVA) using SPSS16 program, and differences were considered statistically significant at p-values <0.05.

4. Conclusion

In this study, a new series of indazolylthiazole moieties was effectively generated and described in a new range of novel pyridine, pyran, furan, thiophene, and pyrazole-carrying compounds. The newly synthesized compounds showed great potency as a selective anticancer drugs against both HepG-2 and Caco-2 cell lines, with high SI values and low IC_{50}values. The antitumor activity of the synthesized derivatives included obvious tumor cell damage and stimulated a clear alteration of the cell morphology in a dose-dependent manner. Among the tested compounds, derivatives 6 and 4 revealed potent antitumor activity, where derivative 8 showed the highest antitumor activity toward both tested tumor cells with SI values of approximately 26 and IC50 values of 5.9 µg/ml, attributed to the presence of a thiazolylpyrazole moiety, with acetonitrile, in the pyrazole ring. The gene expression level study confirmed apoptosis induction through upregulation of the p53 gene (2-8 -fold) in both treated HepG-2 and Caco-2 cells. On the other hand, compound **3** revealed significant broad-spectrum antibacterial activity against *Streptococcus mutans* (MIC of 11.2 µg/ml) and *Pseudomonas aeruginosa* (MIC of 18,29µg/ml), comparable to that of ampicillin MIC (13.5 µg/ml) and ciprofloxacin (18.7µg/ml), which could be attributed to the incorporated thiazolopyridine ring. The newly prepared compounds revealed low to medium antifungal activity against *Candida albicans* with a maximum antifungal activity through compound **3** (36% clotrimazole activity). Many synthesized compounds revealed antibiofilm formation activities (58.5-79%) against the three applied pathogens. Collectively, the results confirmed the effectiveness of newly synthesized compounds as promising antitumor drugs with antimicrobial activity. The current study results encourage our research team to go deeper into the exact antitumor/antimicrobial mechanisms of the newly prepared potent derivatives and explore the structural-functional relationship.

Declarations

Conflicts of interest

The authors declare no potential conflicts of interest with respect to the research, authorship, and/or publication of this article.

Author contributions

N.D. and D.L.: Synthesize the new heterocyclic series, formal analysis, investigation, conceptualization, writing–original draft, supervision. E.M.E.and H.El-G.: evaluating the biological

activties, conceptualization, investigation, writing–review & editing, and visualization. A.E.A.: the molecular docking study, writing, editing and reviewing.

Compliance with Ethical Standards

This article does not contain any studies with human or animal subjects.

References

1. Fahmy, H.H., Srour, A.M., Ismail, M.A., Khater, M.A., Serrya, R.A., El-Manawaty, M.A. Design and synthesis of some new tri-substituted pyrazole derivatives as anticancer agents. Research on Chemical Intermediates., 42, 6881–6892,(2016). https://doi.org/10.1007/s11164-016-2502-2
2. Llovet, J.M., Kelley, R.K., Villanueva, A., Singal, A.G., Pikarsky, E., Roayaie, S., Lencioni, R., Koike, K., Zucman-Rossi, J., Finn, R.S. Hepatocellular carcinoma. Nature Reviews Disease Primers., 7(6) , (2021).https://doi.org/10.1038/s41572-020-00240-3
3. Sawicki, T., Ruszkowska, M., Danielewicz, A. A Review of Colorectal Cancer in Terms of Epidemiology, Risk Factors, Development, Symptoms and Diagnosis. ., Cancers (Basel). 13(9), 2025, (2021). doi: 10.3390/cancers13092025.
4. Yu, Y.M., Cao, Y.S., Wu, Z., Huang, R., Shen, Z.L. Colon metastasis from hepatocellular carcinoma: A case report and literature review. World Journal of Surgical Oncology., 18(1), 189, (2020). https://doi.org/10.1186/s12957-020-01960-2
5. Baffy, G., Brunt, E.M., Caldwell, S.H. Hepatocellular carcinoma in nonalcoholic fatty liver disease: An emerging menace. Journal of Hepatology., 56, 1384–1391,(2012). https://doi.org/10.1016/j.jhep.2011.10.027
6. Sun, B., Karin, M. Obesity, inflammation, and liver cancer. Journal of Hepatology., 56, 704–713, (2012). https://doi.org/10.1016/j.jhep.2011.09.020
7. Llovet, J.M., Ricci, S., Mazzaferro, V., Hilgard, P., Gane, E., Blanc, J.-F., de Oliveira, A.C., Santoro, A., Raoul, J.-L., Forner, A., Schwartz, M., Porta, C., Zeuzem, S., Bolondi, L., Greten, T.F., Galle, P.R., Seitz, J.-F., Borbath, I., Häussinger, D., Giannaris, T., Shan, M., Moscovici, M., Voliotis, D., Bruix, J. Sorafenib in Advanced Hepatocellular Carcinoma. New England Journal of Medicine., 359(4), 378–390,(2008). https://doi.org/10.1056/nejmoa0708857
8. Hirashita, T., Ohta, M., Iwaki, K., Kai, S., Shibata, K., Sasaki, A., Nakashima, K., Kitano, S. Direct invasion to the colon by hepatocellular carcinoma: Report of two cases.World Journal of Gastroenterology., 14, 4583–4585,(2008). https://doi.Org /10 .3748/wjg.14.4583
9. Siegel, R.L., Miller, K.D., Jemal, A. Cancer statistics, 2020. CA: A Cancer Journal for Clinicians., 70, 7–30,(2020). https://doi.org/10.3322/caac.21590
10. Holland, T., Fowler, V.G., Shelburne, S.A. Invasive gram-positive bacterial infection in cancer patients. Clinical Infectious Diseases., 59, S331–S334,(2014). https://doi.org/10.1093/cid/ciu598

11. Abdallah, A.E., Eissa, S.I., Al Ward, M.M.S., Mabrouk, R.R., Mehany, A.B.M., El-Zahabi, M.A. Design, synthesis and molecular modeling of new quinazolin-4(3H)-one based VEGFR-2 kinase inhibitors for potential anticancer evaluation. Bioorganic Chemistry., 109, 104695,(2021). https://doi.org/10.1016/j.bioorg.2021.104695
12. Zhao, M., Cui, Y., Zhao, L., Zhu, T., Lee, R.J., Liao, W., Sun, F., Li, Y., Teng, L. Thiophene derivatives as new anticancer agents and their therapeutic delivery using folate receptor-targeting nanocarriers. ACS Omega., 4(5), 8874–8880,(2019). https://doi.org/10.1021/acsomega. 9b00554
13. Küçükgüzel, Ş.G., Şenkardeş, S. Recent advances in bioactive pyrazoles. European Journal of Medicinal Chemistry., 97, 786–815,(2015). https://doi.org/https://doi.org/10.1016/j.ejmech.2014.11.059
14. Kumar, V., Kaur, K., Gupta, G.K., Sharma, A.K. Pyrazole containing natural products: Synthetic preview and biological significance. European Journal of Medicinal Chemistry., 69,735–753,(2013). https://doi.org/https://doi.org/10.1016/j.ejmech.2013.08.053
15. Sharma, S., Kumar, D., Singh, G., Monga, V., Kumar, B. Recent advancements in the development of heterocyclic anti-inflammatory agents. European Journal of Medicinal Chemistry., 200, 112438, (2020). https://doi.org/10.1016/j.ejmech.2020.112438
16. García-Valverde, M., Torroba, T. Special issue: Sulfur-nitrogen heterocycles. Molecules., 10, 318–320, (2005). https://doi.org/10.3390/10020318
17. Pathania, S., Narang, R. K., Rawal, R. K. Role of sulphur-heterocycles in medicinal chemistry: An update. European Journal of Medicinal Chemistry., 180, 486–508,(2019). https://doi.org/https://doi.org/10.1016/j.ejmech.2019.07.043
18. Singh, P.K., Silakari, O. The Current Status of O-Heterocycles: A Synthetic and Medicinal Overview.Chem Med Chem., 13, 1071–1087,(2018). https://doi.org/10.1002/cmdc.201800119
19. Al-Said, M.S., Bashandy, M.S., Al-Qasoumi, S.I., Ghorab, M.M. Anti-breast cancer activity of some novel 1,2-dihydropyridine, thiophene and thiazole derivatives. European Journal of Medicinal Chemistry., 46, 137–141, (2011). https://doi.org/10.1016/j.ejmech.2010.10.024
20. De Vasconcelos, A., Campos, V.F., Nedel, F., Seixas, F.K., Dellagostin, O.A., Smith, K.R., De Pereira, C.M.P., Stefanello, F.M., Collares, T., Barschak, A.G. Cytotoxic and apoptotic effects of chalcone derivatives of 2-acetyl thiophene on human colon adenocarcinoma cells. Cell Biochemistry and Function., 31, 289–297,(2013). https://doi.org/10.1002/cbf.2897
21. Schmitt, C., Kail, D., Mariano, M., Empting, M., Weber, N., Paul, T., Hartmann, R.W., Engel, M. Design and synthesis of a library of lead-like 2,4-bisheterocyclic substituted thiophenes as selective Dyrk/Clk inhibitors. PLoS ONE., 9,(2014). https://doi.org/10.1371/journal.pone.0087851
22. Harit, T., Bellaouchi, R., Asehraou, A., Rahal, M., Bouabdallah, I., Malek, F. Synthesis, characterization, antimicrobial activity and theoretical studies of new thiophene-based tripodal ligands. Journal of Molecular Structure., 1133, 74–79,(2017). https://doi.org/10.1016/j.molstruc.2016.11.051
23. Sable, P.N., Ganguly, S., Chaudhari, P.D. An efficient one-pot three-component synthesis and antimicrobial evaluation of tetra substituted thiophene derivatives. Chinese Chemical Letters., 25,

1099–1103,(2014). https://doi.org/10.1016/j.cclet.2014.03.044

24. Shahavar Sulthana, S., Arul Antony, S., Balachandran, C., Syed Shafı, S. Thiophene and benzodioxole appended thiazolyl-pyrazoline compounds: Microwave assisted synthesis, antimicrobial and molecular docking studies. Bioorganic and Medicinal Chemistry Letters., 25, 2753–2757,(2015). https://doi.org/10.1016/j.bmcl.2015.05.033
25. Abed, N.A., Hammouda, M.M., Ismail, M.A., Abdel-Latif, E. Synthesis of new heterocycles festooned with thiophene and evaluating their antioxidant activity. Journal of Heterocyclic Chemistry., 57, 4153–4163,(2020). https://doi.org/10.1002/jhet.4122
26. Marques, R., Mendonça-junior, F.J.B., De, M., Scotti, L., Santos, R., Ara, A. De, Reinaldo, N., Almeida, D., Ol, R. Thiophene-Based Compounds with Potential Anti-Inflammatory Activity. Heliyon., 6,(2020). https://doi.org/10.1016/j.heliyon.2020.e05520
27. Mishra, R., Tomar, I., Singhal, S., Jha, K.K. Synthesis, properties and biological activity of thiophene: A review. Der Pharma Chemica., 3(4), 38–54,(2011).
28. Elmetwally, S.A., Saied, K.F., Eissa, I.H., Elkaeed, E.B. Design, synthesis and anticancer evaluation of thieno[2,3-d]pyrimidine derivatives as dual EGFR/HER2 inhibitors and apoptosis inducers. Bioorganic Chemistry., 88, 102944,(2019). https://doi.org/10.1016/j.bioorg.2019.102944
29. Ghith, A., Youssef, K.M., Ismail, N.S.M., Abouzid, K.A.M. Design, synthesis and molecular modeling study of certain VEGFR-2 inhibitors based on thienopyrimidne scaffold as cancer targeting agents. Bioorganic Chemistry., 83, 111–128,(2019). https://doi.org/10.1016/j.bioorg.2018.10.008
30. Gul, H.I., Yamali, C., Sakagami, H., Angeli, A., Leitans, J., Kazaks, A., Tars, K., Ozgun, D.O., Supuran, C.T. New anticancer drug candidates sulfonamides as selective hCA IX or hCA XII inhibitors. Bioorganic Chemistry.,77, 411–419,(2018). https://doi.org/10.1016/j.bioorg.2018.01.021
31. Milik, S.N., Abdel-Aziz, A.K., Lasheen, D.S., Serya, R.A.T., Minucci, S., Abouzid, K.A.M. Surmounting the resistance against EGFR inhibitors through the development of thieno[2,3-d]pyrimidine-based dual EGFR/HER2 inhibitors. European Journal of Medicinal Chemistry., 155, 316–336,(2018). https://doi.org/10.1016/j.ejmech.2018.06.011
32. Shah, R., Verma, P.K. Therapeutic importance of synthetic thiophene. Chemistry Central Journal., 12, 1–22,(2018). https://doi.org/10.1186/s13065-018-0511-5
33. Zhao, M., Cui, Y., Zhao, L., Zhu, T., Lee, R.J., Liao, W., Sun, F., Li, Y., Teng, L. Thiophene derivatives as new anticancer agents and their therapeutic delivery using folate receptor-targeting nanocarriers. ACS Omega., 4, 8874–8880,(2019). https://doi.org/10.1021/acsomega.9b00554
34. Alam, M.J., Alam, O., Alam, P., Naim, M.J. A Review on Pyrazole chemical entity and Biological Activity. International Journal of Pharma Sciences and Research., 6, 1433–1442,(2015).
35. B'Bhatt, H., Sharma, S. Synthesis and antimicrobial activity of pyrazole nucleus containing 2-thioxothiazolidin-4-one derivatives. Arabian Journal of Chemistry., 10, S1590–S1596,(2017). https://doi.org/10.1016/j.arabjc.2013.05.029
36. Mohamed, L.W., Shaaban, M.A., Zaher, A.F., Alhamaky, S.M., Elsahar, A.M. Synthesis of new pyrazoles and pyrozolo [3,4-b] pyridines as anti-inflammatory agents by inhibition of COX-2 enzyme. Bioorganic

Chemistry., 83, 47–54,(2019). https://doi.org/10.1016/j.bioorg.2018.10.014

37. Abdel-Aziz, M., Abuo-Rahma, G.E.D.A., Hassan, A.A. Synthesis of novel pyrazole derivatives and evaluation of their antidepressant and anticonvulsant activities. European Journal of Medicinal Chemistry.,44, 3480–3487,(2009). https://doi.org/10.1016/j.ejmech.2009.01.032
38. Kaushik, D., Khan, S.A., Chawla, G., Kumar, S. N'-[(5-chloro-3-methyl-1-phenyl-1H-pyrazol-4-yl)methylene] 2/4-substituted hydrazides: Synthesis and anticonvulsant activity. European Journal of Medicinal Chemistry., 45, 3943–3949,(2010). https://doi.org/10.1016/j.ejmech.2010.05.049
39. Koca, I., Özgür, A., Coşkun, K.A., Tutar, Y. Synthesis and anticancer activity of acyl thioureas bearing pyrazole moiety. Bioorganic and Medicinal Chemistry., 21, 3859–3865,(2013). https://doi.org/10.1016/j.bmc.2013.04.021
40. Claudio Viegas-Junior, Eliezer J. Barreiro, Carlos Alberto Manssour Fraga. Molecular Hybridization: A Useful Tool in the Design of New Drug Prototypes. Current Medicinal Chemistry., 14, 1829–1852, (2007). https://doi.org/10.2174/092986707781058805
41. El-fakharany, E., Dawoud, N., El-gendi, H., Emara, A., Lottfy, D. Consolidated antimicrobial and anticancer activities through newly synthesized novel series of pyrazoles bearing indazolylthiazole moiety: characterization and molecular docking.Egypt J Chem., 64(11), 6571- 6582,(2021). https://doi.org/10.21608/ejchem.2021.83623.4104
42. Ibrahim, M.F., Abdel-Reheem, H.A., Khattab, S.N., Hamed, E.A. Nucleophilic Substitution Reactions of 2,4-Dinitrobenzene Derivatives with Hydrazine: Leaving Group and Solvent Effects. International Journal of Chemistry., 5, 33–45,(2013). https://doi.org/10.5539/ijc.v5n3p33
43. Ghorab, M.M., Al-Said, M.S. Anticancer activity of novel indenopyridine derivatives. Archives of pharmacal research., 35, 987–994,(2012). https://doi.org/10.1007/s12272-012-0605-x
44. Abdel Reheim, M.A.M., Baker, S.M. Synthesis, characterization and in vitro antimicrobial activity of novel fused pyrazolo[3,4-c]pyridazine, pyrazolo[3,4-d]pyrimidine, thieno[3,2-c]pyrazole and pyrazolo[3',4':4,5]thieno[2,3-d]pyrimidine derivatives. Chemistry Central Journal., 11, 112,(2017). https://doi.org/10.1186/s13065-017-0339-4
45. Thomas, J., Jecic, A., Vanstreels, E., van Berckelaer, L., Romagnoli, R., Dehaen, W., Liekens, S., Balzarini, J. Pronounced anti-proliferative activity and tumor cell selectivity of 5-alkyl-2-amino-3-methylcarboxylate thiophenes. European journal of medicinal chemistry., 132, 219–235,(2017). https://doi.org/10.1016/j.ejmech.2017.03.044
46. Mohareb, R.M., ABDALLAH, A.E.M., AHMED, E.A. Synthesis and cytotoxicity evaluation of thiazole derivatives.Acta Pharm., 67(4), 495-510,(2017).doi: 10.1515/acph-2017-0040..
47. Shaker, S.A., Marzouk, M.I., 2016. Utilization of cyanoacetohydrazide and oxadiazolyl acetonitrile in the synthesis of some new cytotoxic heterocyclic compounds. Molecules., 21(2),155,(2016). https://doi.org/10.3390/molecules 21020155 .
48. Khodairy, A. Synthesis of fused and spiro heterocyclic compounds derived from 3,5-pyrazolidinedione derivatives. Phosphorus, Sulfur and Silicon and Related Elements., 60, 159–180, (2000). https://doi.org/10.1080/10426500008043678

49. Mamidala, S., Aravilli, R.K., Ramesh, G., Khajavali, S., Chedupaka, R., Manga, V., Vedula, R.R. A facile one-pot, three-component synthesis of a new series of thiazolyl pyrazole carbaldehydes: In vitro anticancer evaluation, in silico ADME/T, and molecular docking studies. Journal of Molecular Structure., 1233, 130111,(2021). https://doi.org/10.1016/j.molstruc.2021.130111
50. Matiadis, D., Sagnou, M. Pyrazoline hybrids as promising anticancer agents: An up-to-date overview. International Journal of Molecular Sciences., 21, 1–41,(2020). https://doi.org/10.3390/ijms21155507
51. Sayed, A.R., Gomha, S.M., Abdelrazek, F.M., Farghaly, M.S., Hassan, S.A., Metz, P. Design, efficient synthesis and molecular docking of some novel thiazolyl-pyrazole derivatives as anticancer agents. BMC Chemistry., 13, 1–13,(2019). https://doi.org/10.1186/s13065-019-0632-5
52. Lang, S.J., Schmiech, M., Hafner, S., Paetz, C., Steinborn, C., Huber, R., Gaafary, M. El, Werner, K., Schmidt, C.Q., Syrovets, T., Simmet, T. Antitumor activity of an Artemisia annua herbal preparation and identification of active ingredients. Phytomedicine : international journal of phytotherapy and phytopharmacology., 62, 152962,(2019). https://doi.org/10.1016/j.phymed.2019.152962
53. Lee, J., Choi, B.U.Y., Keum, Y.S.A.M., 2017. Acetonitrile extract of Salvia miltiorrhiza Radix exhibits growth-inhibitory effects on prostate cancer cells through the induction of cell cycle arrest and apoptosis. Oncol Lett., 13(5):2921-2928,(2017). https://doi.org/10.3892/ol.2017.5820
54. Matly, A., Quinn, J.A., Mcmillan, D.C., Park, J.H., Edwards, J. The relationship between β -catenin and patient survival in colorectal cancer systematic review and meta-analysis. Critical Reviews in Oncology / Hematology., 163, 103337,(2021). https://doi.org/10.1016/j.critrevonc.2021.103337
55. Gu, J., Zhang, L., Swisher, S.G., Liu, J., Roth, J.A., Fang, B. Induction of p53-regulated genes in lung cancer cells: Implications of the mechanism for adenoviral p53-mediated apoptosis. Oncogene., 23, 1300–1307,(2004). https://doi.org /10.1038 /sj.onc. 1207239
56. Hematol, J., Hu, J., Cao, J., Topatana, W., Juengpanich, S., Li, S., Zhang, B., Shen, J. Targeting mutant p53 for cancer therapy : direct and indirect strategies. Journal of Hematology & Oncology., 14(157), 1–19,(2021). https://doi.org/10.1186/s13045-021-01169-0
57. Shao, J., Zhang, Q., Wei, J., Yuchi, Z., Cao, P., Li, S.-Q., Wang, S., Xu, J.-Y., Yang, S., Zhang, Y., Wei, J.-X., Tian, J.-L. Synthesis, crystal structures, anticancer activities and molecular docking studies of novel thiazolidinone Cu(ii) and Fe(iii) complexes targeting lysosomes: special emphasis on their binding to DNA/BSA. Dalton Trans., 50, 13387–13398,(2021)https://doi.org/10.1039/D1DT02180J
58. Graham, T.A., Ferkey, D.M., Mao, F., Kimelman, D., Xu, W. Tcf4 can specifically recognize β-catenin using alternative conformations. Nature Structural Biology., 8(12), 1048-52 8., 1048–1052,(2001). https://doi.org/10.1038/nsb718
59. Poy, F., Lepourcelet, M., Shivdasani, R.A., Eck, M.J. Structure of a human Tcf4- β-catenin complex. Nature Structural Biology., 8(12), 1053-7,(2000). doi: 10.1038/nsb720. 8, 1053–1057. https://doi.org/10.1038/nsb720
60. Iyer, S., Darley, P.I., Acharya, K.R. Structural insights into the binding of vascular endothelial growth factor-B by VEGFR-1D2: Recognition and specificity. Journal of Biological Chemistry., 285, 23779–

23789,(2010). https://doi.org/10.1074/jbc.M110.130658

61. Feng, X., Jin, S., Wang, M., Pang, Q., Liu, C., Liu, R., Wang, Y., Yang, H., Liu, F., Liu, Y. The Critical Role of Tryptophan in the Antimicrobial Activity and Cell Toxicity of the Duck Antimicrobial Peptide DCATH. Frontiers in Microbiology., 11, 1–14,(2020). https://doi.org/10.3389/fmicb.2020.01146
62. Lozynskyi, A. V., Derkach, H.O., Zasidko, V. V., Konechnyi, Y.T., Finiuk, N.S., Len, Y.T., Kutsyk, R. V., Regeda, M.S., Lesyk, R.B. Antimicrobial and cytotoxic activities of thiazolo[4,5-b]pyridine derivatives. Biopolymers and Cell., 37, 153–164,(2021). https://doi.org/10.7124/bc.000A53
63. Khidre, Rizk E., Radini, I.A.M. Design, synthesis and docking studies of novel thiazole derivatives incorporating pyridine moiety and assessment as antimicrobial agents. Scientific Reports., 11,7846, (2021). https://doi.org/10.1038/s41598-021-86424-7
64. Di Somma, A., Moretta, A., Canè, C., Cirillo, A., Duilio, A., 2020. Inhibition of Bacterial Biofilm Formation. Bacterial Biofilms 1–11. https://doi.org/10.5772/intechopen.9061
65. Mosmann, T. Rapid colorimetric assay for cellular growth and survival: application to proliferation and cytotoxicity assays. Journal of immunological methods., 65, 55–63,(1983). https://doi.org/10.1016/0022-1759(83)90303-4
66. Abu-Serie, M.M., El-Fakharany, E.M. Efficiency of novel nanocombinations of bovine milk proteins (lactoperoxidase and lactoferrin) for combating different human cancer cell lines. Scientific Reports., 7(1),(2017). https://doi.org/10.1038/s41598-017-16962-6
67. Uversky, V.N., El-Fakharany, E.M., Abu-Serie, M.M., Almehdar, H.A., Redwan, E.M. Divergent Anticancer Activity of Free and Formulated Camel Milk α-Lactalbumin. Cancer Investigation., 35, 610–623, (2017). https://doi.org/10.1080/07357907.2017.1373783
68. El-Fakharany, E.M., Abu-Serie, M.M., Litus, E.A., Permyakov, S.E., Permyakov, E.A., Uversky, V.N., Redwan, E.M. The Use of Human, Bovine, and Camel Milk Albumins in Anticancer Complexes with Oleic Acid. Protein Journal., 37, 203–215,(2018). https://doi.org/10.1007/s10930-018-9770-1

Scheme

Schemes 1 and 2 are available in the Supplementary Files section

Figures

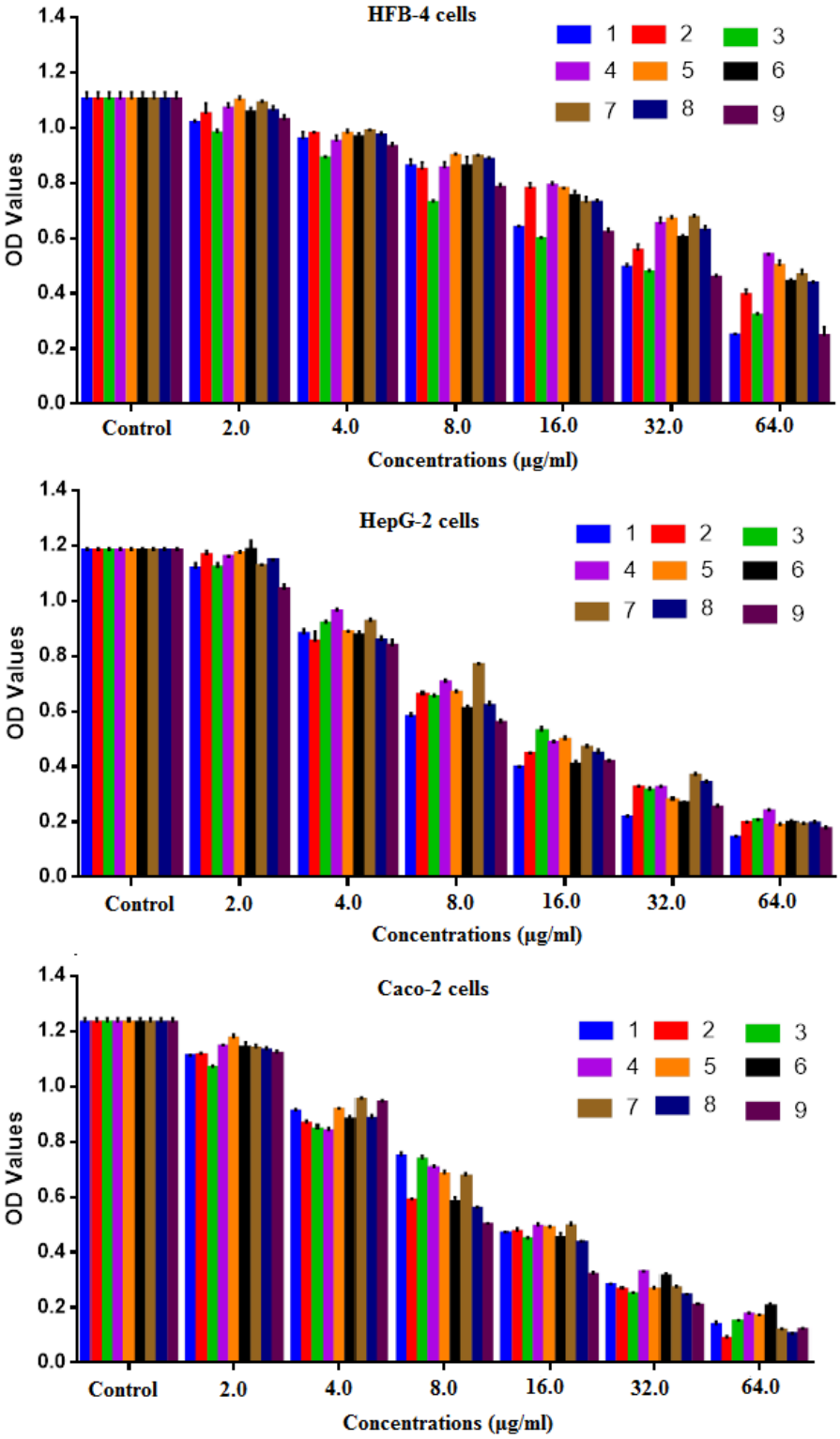

Figure 1

Effect of the prepared derivatives on the cell viability of the human normal (HFB-4) cells and human cancer (HepG-2 and Caco-2) cell lines after treatment for 48 h compared to untreated cells (expressed as triplicate values mean±SEM).

Figure 2

In vitro effect of the prepared derivatives on the morphological alterations of HepG-2 cells (A) and Caco-2 cells (B) as observed under a phase-contrast microscope. Both HepG-2 and Caco-2 cells were treated with synthetic compounds (**4**, **6,** and **8**) at various concentrations for 48 h and compared to untreated cells (control).

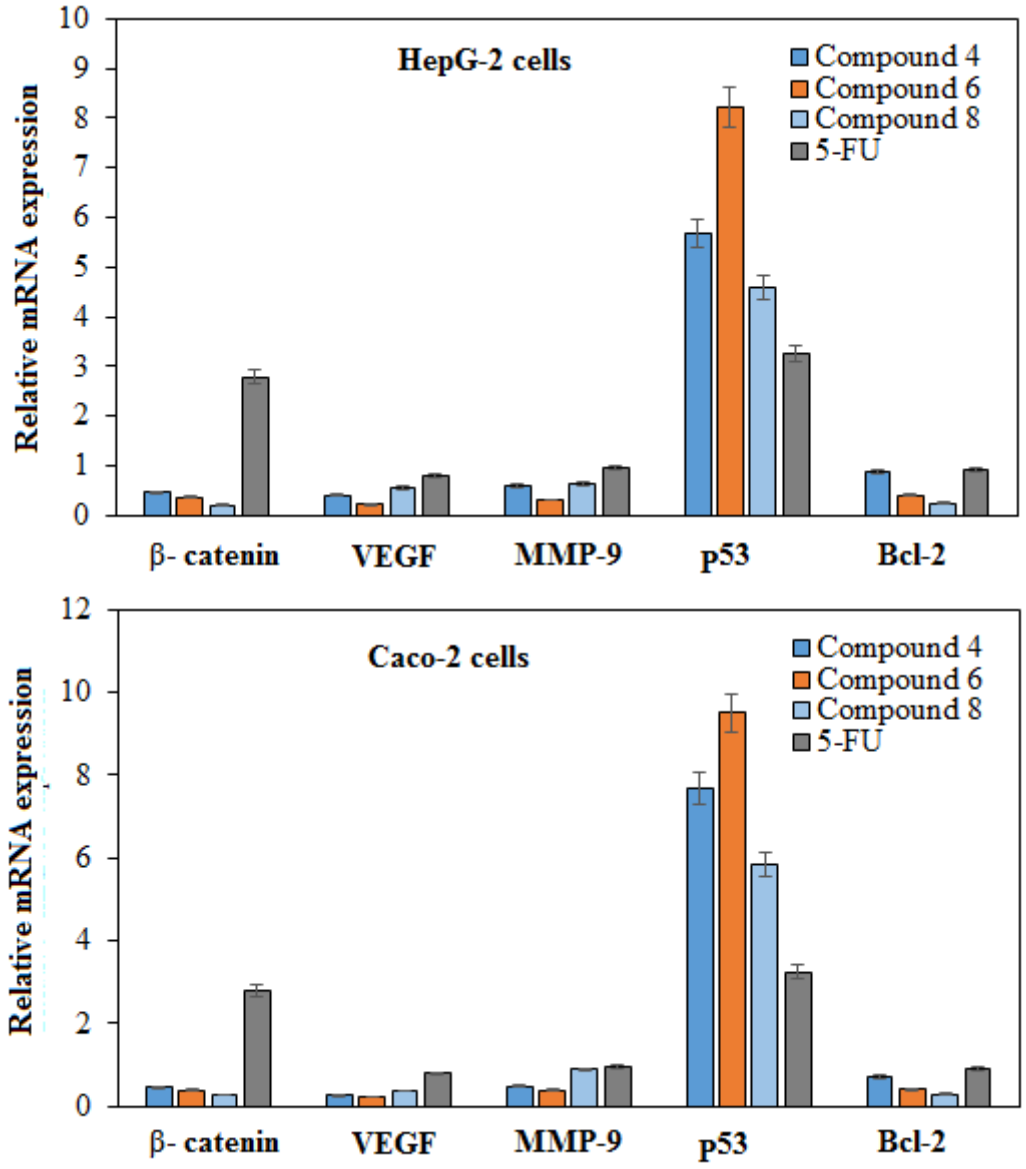

Figure 3

Evaluating the relative changes in mRNA expression levels of five key genes (β-catenin, VEGF, MMP-9, p53, and Bcl-2) in HepG-2 and Caco-2 cells treated with potent antitumor synthesized compounds

compared to 5-FU standard anticancer drug.

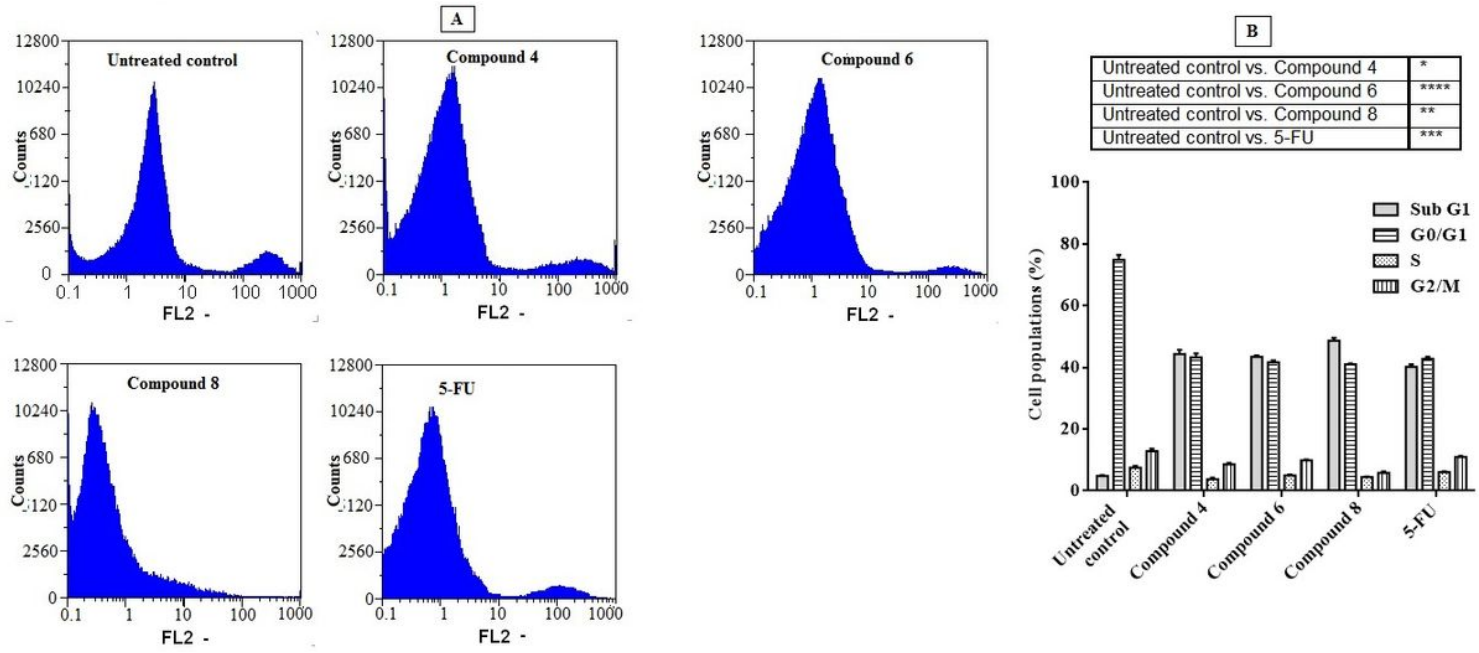

Figure 4

Cell cycle distribution analysis of Caco-2 cells treated with the potent antitumor synthesized compounds compared to 5 FU standard anticancer drug for 48 h, (A) original flow charts of cell cycle diagrams and (B) quantitative distribution of the treated cells in cell cycle phases compared with control (untreated) cells. Each bar represents the mean ± SEM (n = 3) and *p < 0.05, **p < 0.01, ***p < 0.001 and ****p < 0.0001 vs. untreated control.

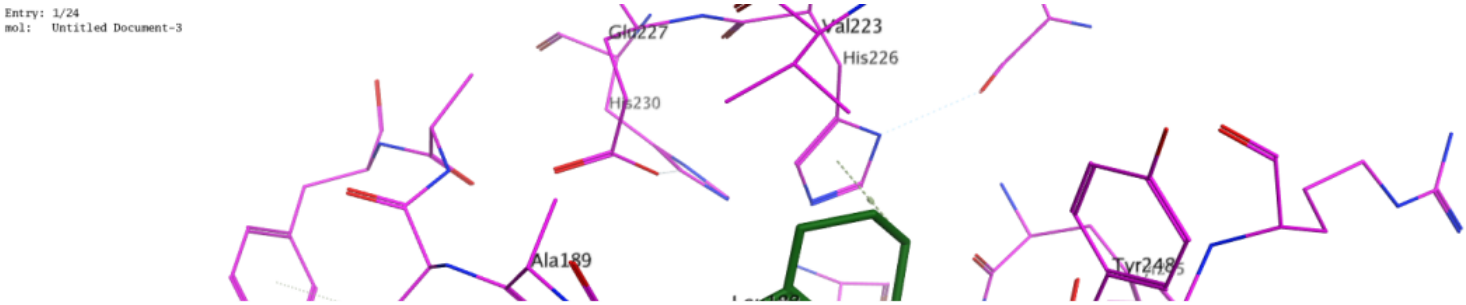

Figure 5

3D illustration of possible ligand interactions with MM-9 protein (PDB ID 4XCT).

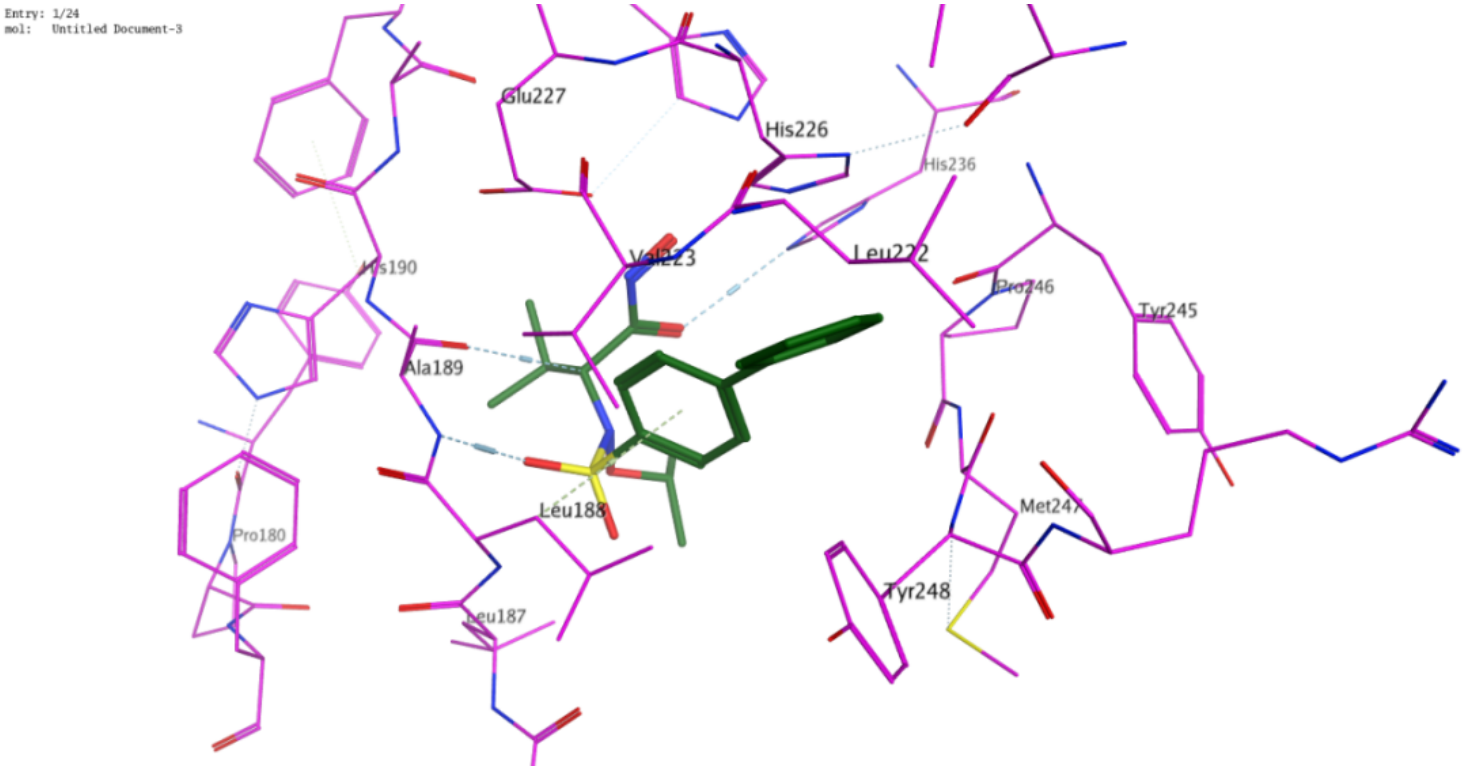

Figure 6

3D illustration of possible interactions of compound **4** with MMP-9 protein (PDB ID 4XCT).

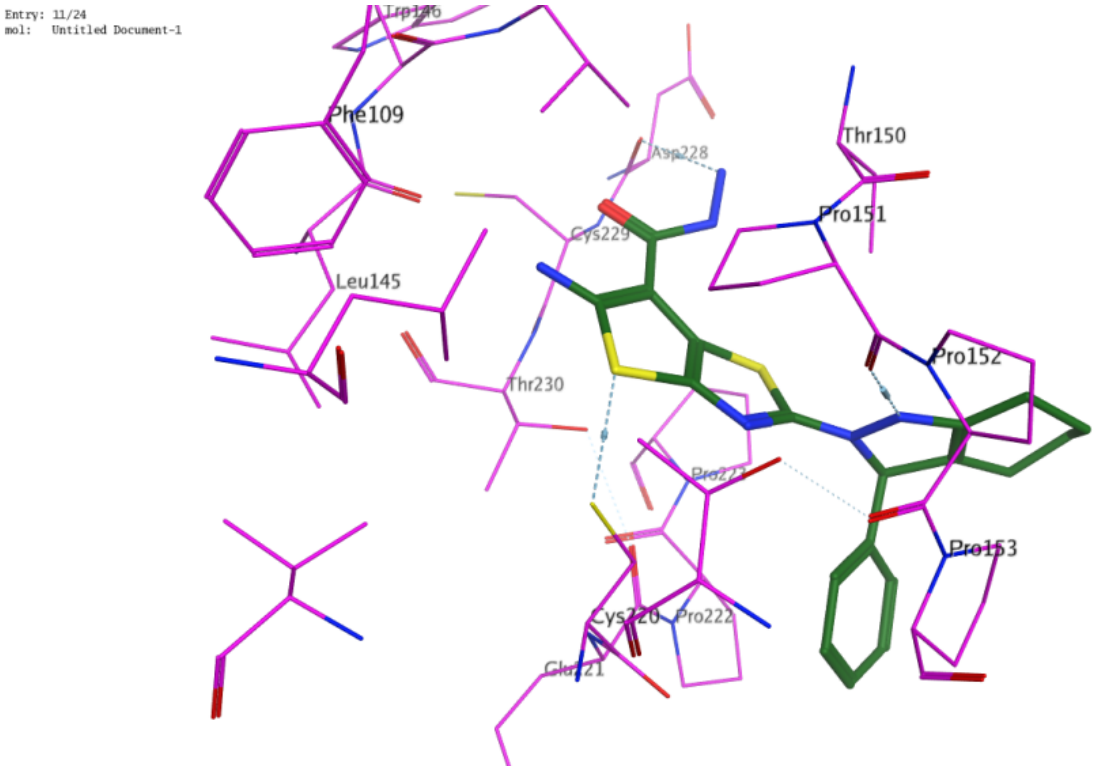

Figure 7

3D illustration of possible interactions of compound **6** with p53 protein (PDB ID 3ZME).

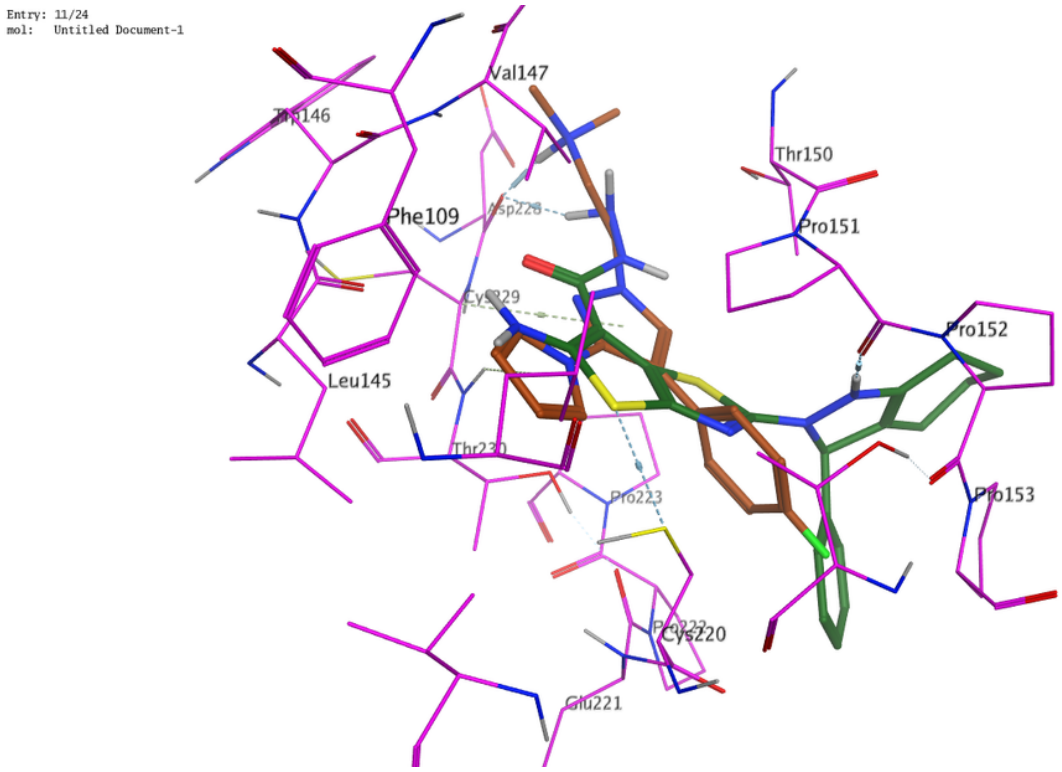

Figure 8

3D illustration of the overlay of compound **6** (green colored) and the ligand (brown colored) into p53 (PDB ID 3ZME).

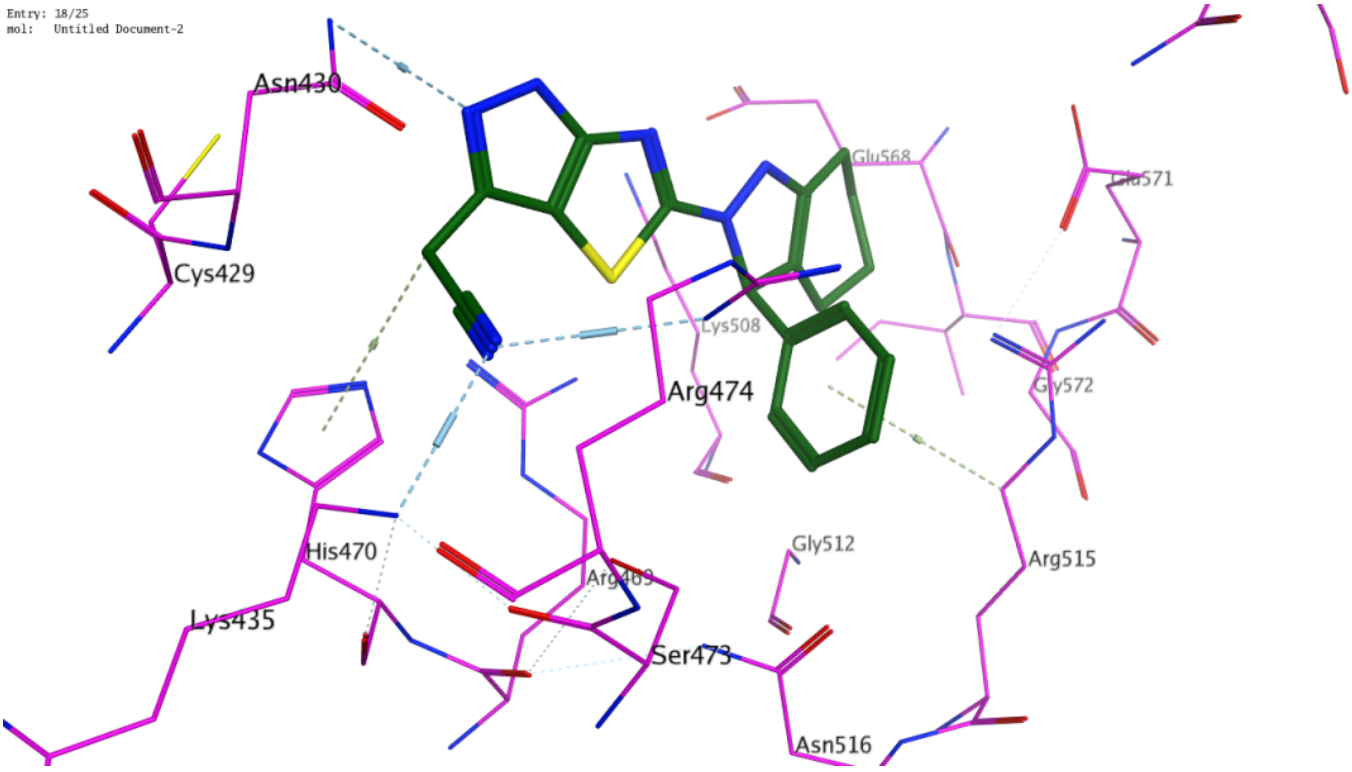

Figure 9

3D illustration of possible interactions of compound **8** with β-catenin protein (PDB ID 1JDH).

Figure 10

3D illustration of possible interactions of compound **6** with β-catenin (PDB ID 1JDH).

Figure 11

3D illustration of possible interactions of compound **6** with VEGF protein (PDB ID 2XAC).

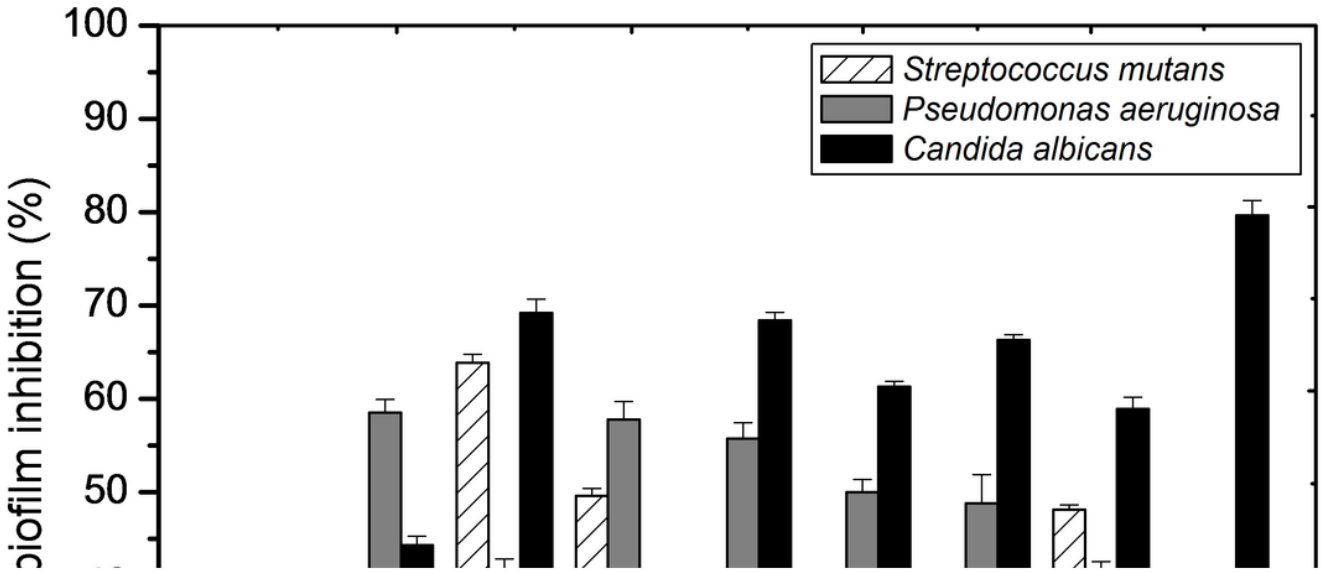

Figure 12

Efficacy of the newly prepared compounds (1-9) on microbial biofilm inhibition against three human pathogens: *Streptococcus mutant, Pseudomonas aeruginosa,* and *Candida albicans.*

Supplementary Files

This is a list of supplementary files associated with this preprint. Click to download.

- paperf2.docx
- scheme1.png

- scheme2.png